Specific defects, surface band bending and characteristic green emissions of ZnO

Y. Y. Tay,[ab] T. T. Tan,[a] M. H. Liang,[b] F. Boey[b] and S. Li*[a]

Received 15th December 2009, Accepted 3rd March 2010
First published as an Advance Article on the web 9th April 2010
DOI: 10.1039/b926427b

The green emission in ZnO can be identified as two characteristic emissions, namely high and low energy emissions, respectively. The study of band bending effect of ZnO surface demonstrates that oxygen vacancies cause both the core level and the valence band to shift to higher binding energy. The downward band bending induced by a strong accumulation layer, where the oxygen vacancies act as donors, results in the high energy green emission. ZnO with the low energy green emission has Zn 2p 3/2 core level binding energy shifted to lower binding energy. The depth of dominant oxygen vacancies plays an important role in determining the mechanisms of green emission.

Introduction

ZnO has attracted enormous interest in the past decade due to its newly discovered properties as well as the possibility of manipulating its properties in conjunction with the emerging nanoscale applications,[1] such as nanoelectronic devices and UV photodetectors, and nano-lasers.[2–4] ZnO can also be the host material in which the residing electrons can travel over a longer distance, yet remain unscattered with the quantum Hall effect incorporated into the versatile functionality of metal oxides in complex heterostructures.[4] However, such possible applications require stringent fabrication methodology to achieve ultra-high purity materials with minimal defects. There is also a great field of interest in the doping of ZnO, due to the many interesting properties observed.[5–8]

Photoluminescence spectroscopy is one of the characterization techniques that determine the defects in wide bandgap semiconductors. ZnO normally emits a strong UV light, which is an exciton emission. Very often, other emissions in the green, yellow and orange region can be observed and these are known to be defect related.[9] However, challenges still remain in the identification of the exact defects that give rise to the respective emission phenomena. In particular, the origin of the green emission remains the most debatable. It has been suggested that oxygen vacancies (donor) in the form of a singly ionized V_o^+ center[10] or a doubly ionized V_o^{++} center[11] is the dominant factor for green emission. Recent investigations suggested that the green emission may also be associated with zinc vacancies[12] (acceptor) or interstices.[13] Such varieties of mechanisms contribute to the diverse emission spectra of green emission with peak emission wavelengths ranging from ~510 nm (~2.43 eV)[10] to ~550 nm (~2.25 eV).[11] The variation may appear deceptively insignificant since, after all, it is still within the domain of green, and the instrument configuration could also have contributed to this subtleties.[14] While it has often been erroneously assumed that the defects formed are homogeneously distributed, it had been noted that some specific defects were confined more to the surface.[15,16]

Recently the correlation between the characteristic green emissions and specific defects of ZnO was investigated through a series of experiments that were designed to separate the subtle interplays among the various types of specific defects.[17] The results demonstrate that the observed green emissions can be identified as two types of individual emissions, namely high energy and low energy, that are associated with the specific defects and their locations. The observation with High Resolution Transmission Electron Microscopy and X-ray Photoelectron Spectroscopy (XPS) revealed that the surface modification caused by the oxygen vacancies on the utmost surface (Type I defects) is responsible for the high energy green emission. The relationship between the intensity of the low energy green emission and the crystallographic lattice contraction indicates that oxygen vacancy is the dominant of such an emission that resides within the bulk of ZnO (Type II defects).

Unlike the transition metals that would have multiple ion valence states, Zn only have limited ion valence states *e.g.* +1 and +2.[18] This suggests that it is very difficult to quantitatively determine the variation of chemical compositions caused by the processing in different atmospheres with the state-of-the-art characterization techniques. This is true as the phase diagram of ZnO shows an extremely narrow range of possible chemical composition (*e.g.* atomic percent of Zn change is less than 0.0001%).[19] Nevertheless, the work done on XRD has shown some qualitative results which are related to the presence of Type I and Type II defects. However, the processing temperature dependence of ZnO lattice constants was only observed in the materials with Type II defects. This phenomenon can be correlated to the relative intensity of the lower energy green emission, suggesting that Type II defects are found beneath the surface.

In this work, we determine that the subtle variations of the green emissions are substantial to warrant two different intrinsic origins. The mechanism of the surface band bending caused by the specific defects and the underlying chemical physics are studied in detail.

[a] *School of Materials Science and Engineering, The University of New South Wales, NSW 2052 Australia. E-mail: sean.li@unsw.edu.au*
[b] *School of Materials Science and Engineering, Nanyang Technological University, Singapore 639798*

Experimental

The as-received ZnO (99.5% pure, Analyticals Carlo Erba) has an average particle size of 175 ± 35 nm. To separate the subtle changes in the visible emission, the specific defects were induced artificially under two different conditions. In the first condition, Type I defects were induced through annealing the as-received ZnO powder in a reducing atmosphere of 3% H_2 + 97% Ar from 500 °C to 900 °C for 24 h. In the second condition, the Type II defects were generated in ambient atmosphere. This atmosphere could be considered a mixture of 21% O_2 + 79% N_2. Both annealing conditions mentioned above were subsequently subjected to a cooling rate of 100 °C h^{-1}. Photoluminescence (PL) spectra were determined by an Accent Rapid Photoluminescence Mapping System with a He–Cd laser source (325 nm). A constant power of 1.8 mW was maintained to eliminate the possibility of UV to defect emission intensity ratio variation. X-Ray Photoelectron Spectroscopy (XPS) was performed with 20 eV pass energy and the results were subsequently calibrated by adventitious carbon C 1s peak at 285 eV. The Valence-Band Maximum (VBM) with respect to the Fermi-level is determined by extrapolating a linear fit to the leading edge of the valence-band photoemission to the background level.[20]

Results and discussions

Fig. 1(a) shows the variation of the green emission resulting from the Type I and Type II defects. The high energy green emission caused by Type I defects has a peak energy of 2.46 eV (~504.4 nm) while the low energy green emission induced by the Type II defect has a peak energy of ~2.26 eV (~549.0 nm). To illustrate that the energy shift is indeed a consequence of the Type I defects rather than the hydrogen doping, a pristine ZnO sample was processed in a nitrogen atmosphere with the same parameters. The resultant peak shift is identical to that of the sample with the Type I defects as shown in Fig. 1(b). It rules out the contribution of hydrogen.

The relative intensities of these green emissions normalized to their respective UV emissions increase as a function of the processing temperature. The relative intensity of the green emission is related to the concentration of the specific defects acting as the emission center. The correlation among the intensity of green emission, concentration of defects, processing temperatures and environments were investigated by the PL spectroscopy and crystallographic structural characterization using X-ray diffraction.[17] The results showed that, in an ambient environment, the unit cell volume was shrunk as the processing temperature increases. This was associated with the increase of the concentration of Type II defects, which have defect behavior in the bulk. However, such a phenomenon is not the case when ZnO was processed in a reducing environment with Type I defects. It has been experimentally demonstrated that the dominant defects, which are responsible for the higher energy green emission, are associated with surface modification. Fig. 2 shows the core level and valence band binding energy shift as a function of the relative intensity of the characteristic green emissions for the materials with Type I and Type II defects respectively. For the ZnO with Type I defects, the Zn 2p 3/2 core level binding energy shifts gradually to higher binding energy from 1021.1 eV to 1023.0 eV as the relative intensity of high energy green emission increases from R = 1.66 to R = 7.08 [Fig. 2(a)]. A similar correlation between shifting of the VBM and the relative intensity of high energy green emission is also observed experimentally in Fig. 2(b).

Different from the phenomena observed in ZnO with Type I defects, the Zn 2p 3/2 core level binding energies generally decrease with increasing relative intensity of the low energy green emission in the ZnO with Type II defects. It is interesting to note that while Zn 2p 3/2 core level binding energies shifted to lower energy, the VBM shifted to higher binding energy. This is distinct from [Fig. 2(b)] that of ZnO with Type I defects.

Such phenomena may be explained with the characterization of XPS results within the framework of the surface band bending mechanism.[21] Fig. 3 shows the schematic diagrams of the surface band bending mechanism interpreted by core level binding energy or VBM in XPS. For a hypothetical semiconductor with an absent of band bending, the VBM hypothetically determined from XPS has an energy of χ eV from the Fermi level, E_F = 0 eV as shown in Fig. 3(a). On the other hand, this VBM can be represented as a horizontal red dotted line in the band diagram shown in Fig. 3(b). This red dotted line represents the flat band condition from the bulk to the surface for this hypothetical semiconductor. We assume an n-type semiconductor has a Fermi level pinned to the surface and its VBM in XPS [Fig. 3(a)] (now shifted γ eV away from

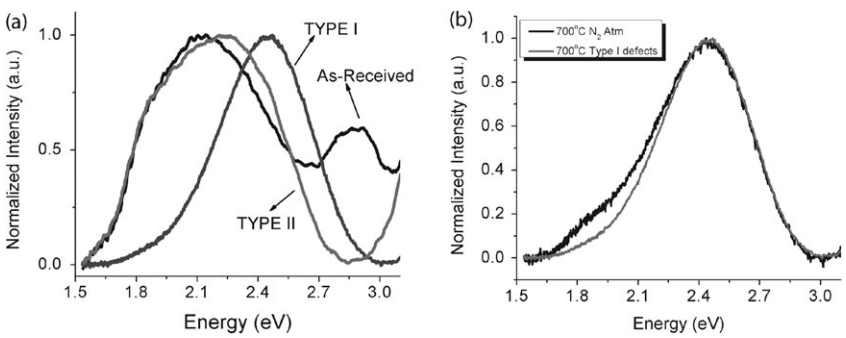

Fig. 1 (a) The ZnO with Type I and Type II defects of high and low energy green emission of ZnO which are annealed at 700 °C, respectively. (b) ZnO annealed under a nitrogen atmosphere shows similar high energy green emission.

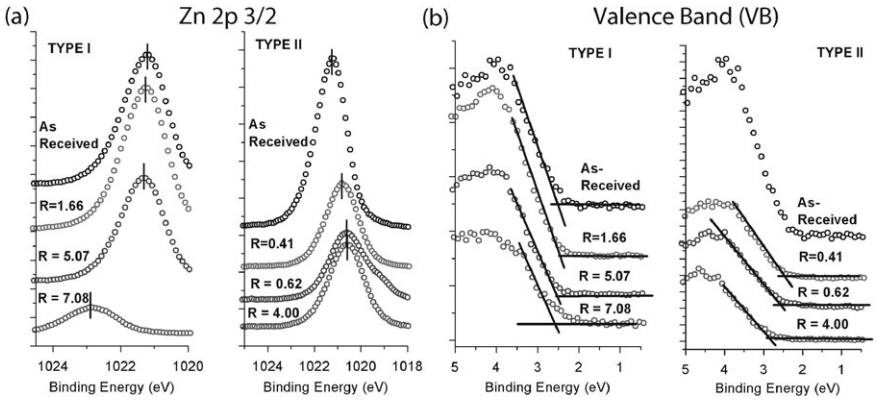

Fig. 2 (a) Zn 2p 3/2 core level binding energy of ZnO with Type I and Type II defects. The relative green emission intensity with respect to the UV emission is denoted as 'R'; (b) valence band maximum (VBM) of ZnO with Type I and Type II defects.

E_F, where $\gamma > \chi$ in value. Therefore, its VBM (as represented by the black continuous line) as shown in the band diagram of Fig. 3(b) would shift downwards from the E_F by γ eV [Fig. 3(b)]. It is noted that γ eV, which is the amount of band bending, is found at a probing depth of σ determined by the XPS [Fig. 3(b)]. Such downward band bending indicates an accumulation of electrons contributed by donor defects near the surface for an n-type material. Likewise, if the binding energy shifts towards the E_F, it would indicate the formation of a surface depleted of electrons, thus an upward bending would be observed. The effects of accumulation or depletion layer not only influence the VBM but also the core level binding energy in a similar manner.[22] The nature of the surface band bending is also influenced by the absorption of atoms or molecules of interest.[23,24] It is therefore noted that the as-received ZnO absorbed moisture from the environment, thus having a hydroxylated surface. Through a reaction of $H + O^{2-} \rightarrow OH^- + e^-$, a shallow donor state may be formed to allow a many-fold increase in the carrier concentration on the space charge layer. This implies that the as-received sample most likely would have an accumulation layer.[25]

The surface banding phenomenon also requires the probing depth of XPS to be considered because the X-ray source with certain energy has a fixed maximum probing depth that is dependent on the binding energy of the electron orbitals (or VBM) for that particular material. The electron's inelastic mean free path (IMFP), α, could be estimated at the particular binding energy using the Tanuma, Powell, and Penn TPP2M formula.[26] The maximum sampling depth was derived from the decaying function of $\exp[-d/\alpha]$,[27] where d is the approximated sampling depth. Since d is approximated by 3α, in this depth $\sim$95% of all the photoelectrons would be scattered by the time they reach the surface. Therefore, the calculation shows that the estimated maximum sampling depth for Zn 2p 3/2 is approximately 3.48 nm while it is approximately $\sim$8.18 nm for the VBM region.

The ZnO with Type I defects induced at 900 °C has its core level Zn 2p 3/2 shifted to a higher binding energy by 1.9 eV while its VBM shifted to higher energy by only 0.35 eV with reference to the as-received ZnO. Therefore, the downwards surface band bending is more severe at a shallower depth. The overview of the core level as well as the VBM shift in the form of surface band bending is illustrated in Fig. 4(a). Such a surface band bending effect indicates that the active donor concentration is dominant in the surface layer ($\sim$3.48 nm) but reduces along the depth and finally reaches the concentration of the bulk. It has been reported that an accumulation of electron near the surface layers may be associated with oxygen vacancies, V_o which is an electron donor [Fig. 4(b)].[16]

The observation of VBM and the core level shift for the ZnO with Type II defects is more complex. The Zn 2p 3/2 core level has a shallower probing depth ($\sim$3.48 nm) and yields a lower binding energy as reference the as-received ZnO [Fig. 4(a)]. Therefore, the degree of downwards band bending

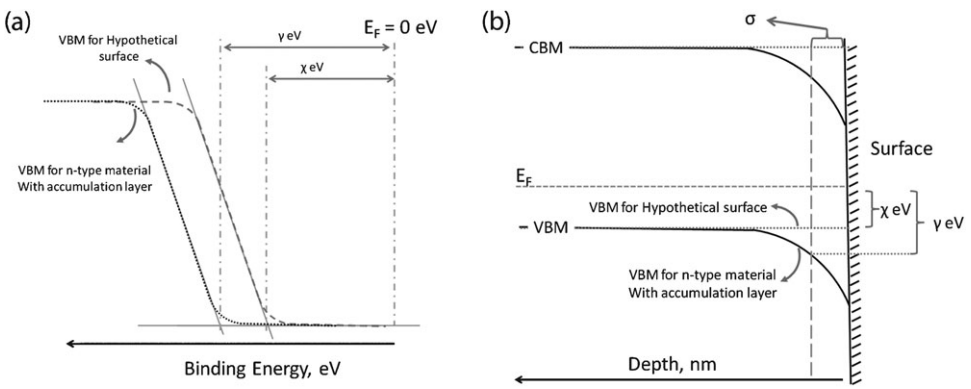

Fig. 3 Schematic diagram of the relationship between (a) XPS using valence band maximum and (b) downwards surface band bending.

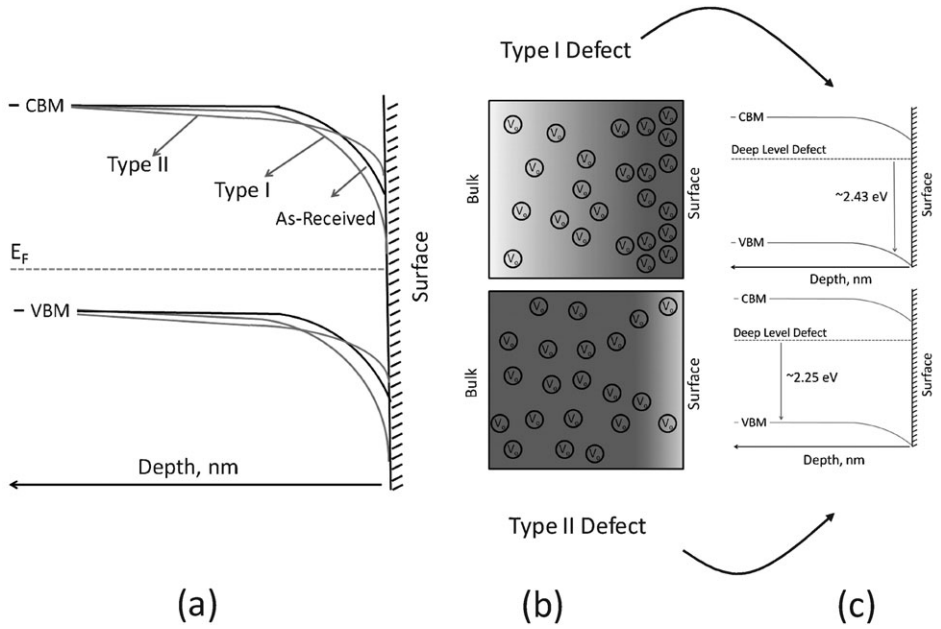

Fig. 4 (a) Schematic diagram of downwards band bending of ZnO with Type I and Type II defects annealed at 700 °C. (b) Schematic diagram of ZnO with the location of Type I and II defects. (c) Electronic transition of Type I and II defects that give rise to the high and low energy green emission respectively.

in this particular material is lower. Compared with the materials processed in both hydrogen and nitrogen, the relatively high oxygen partial pressure at ambient atmosphere resulted in a lower concentration of oxygen vacancies near the surface. Therefore, the electron concentration from the oxygen vacancies (defect donor) is lower due to the compensation of the holes associated with the acceptors. On the other hand, due to the rather rapid cooling at the end of the processing procedures, dramatic reduction of the defect migration rate causes non-uniform distribution of the defects from the surface along the depth [Fig. 4(b)] and this spans a distance of around 10 nm.[28] This led the oxygen vacancies to be more dominant at a deeper depth (~8.18 nm) onwards [Fig. 4(b)]. As a result the donor/electron concentration increase beneath the surface and consequently, the VBM shifted to a higher energy as compared to that of the as-received ZnO. Although the mechanism of defect migration in such cases is unclear, such phenomenon has been observed by others.[28]

In Fig. 4(c), we separate the surface band banding for the ZnO with Type I and II defects. The aforementioned Type I defects should be the oxygen vacancies that are concentrated near the surface, thus resulting in the downwards surface band bending. Since the oxygen vacancies are a deep level defect of localized state, the band bending effect should have little influence in altering its energetic position as compared to those shallow donor/acceptors.[11] Hence, the electronic transition from the deep level state to the VBM occurs at a higher energy, giving rise to high energy green emission. On the other hand, oxygen vacancies which are mostly present in the bulk should be the Type II defects such that low energy green emission occurs in the flat band region. Fig. 5 shows the emission spectra of ZnO annealed in pure oxygen atmosphere and the one with Type II defects as reference, respectively. For the ZnO annealed in the pure oxygen atmosphere, a yellow emission is observed at 2.186 eV which is not in the green emission range. In our experiments, the zinc partial pressure is similar regardless the processing atmosphere. Therefore, the variation of the emission spectra indicates that the zinc vacancies are not responsible for the emission behaviors while the oxygen vacancies and their locations are the dominants.

The nature of the core level binding energy as well as the VBM shift could also be affected by several factors. The first is a chemical shift associated with the nature of the chemical bonding state.[27] Since ZnO doesn't have multiple oxidation states, the charge transfer is associated with the change of coordination number. It was reported that the 3d 5/2 core level binding energy of Rh ions shifts to higher binding energy when the coordination number to oxygen increases. This electron charge transfer that causes the higher binding energy shift is consistent with the valence band region.[29] Such a chemical shift is not observed in the ZnO with Type I defects where the surface has a number of oxygen vacancies. It is also unlikely to

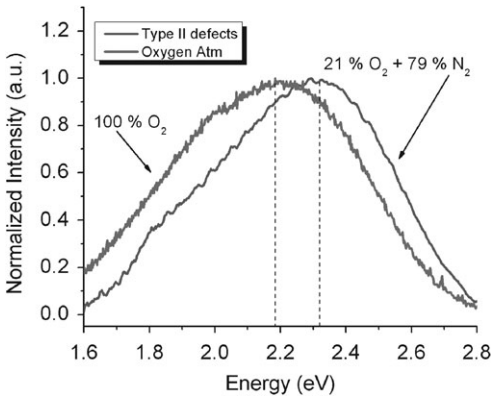

Fig. 5 PL of ZnO annealed under O_2 atmosphere and with Type II defects annealed at 900 °C for 24 h respectively.

Table 1 O 1s core level binding energies of ZnO with Type I and Type II defects with their respective green emissions of increasing relative intensities. The first row contains the necessary information on the as-received sample

Type I defect, relative green emission	Type II defect, relative green emission	O 1s (TYPE I, eV)	O 1s (TYPE II, eV)
—	—	530.1	530.1
1.66	0.41	530.1	529.9
5.07	0.62	530.3	529.7
7.08	4	530.4	529.8

apply this chemical shift to the ZnO with Type II defects as the Zn 2p 3/2 core level shifts to lower energy while Zn 3d core level and VBM shifted to higher binding energy.

The Madelung energy is another factor that plays a role in the core level shift. For metal ions with higher coordination number, the Madelung energy component lowers its binding energy shift, while the binding energy of oxygen ions shifts to higher energy.[30] Table 1 shows the O 1s binding energy of ZnO with the high and low energy green emissions that are associated with Type I and Type II defects respectively. For the ZnO with Type I defects, the O 1s generally increases in its binding energy which shares the same trend as the Zn 2p 3/2 core level. For the ZnO with Type II defects, the O 1s core level binding energy generally shifts to lower binding energy, similar to the Zn 2p 3/2 core level binding energy. However, neither of these materials shows the Madelung energy to be dominant. The above considerations favor our assignment of the binding energy to the observation of band bending.

For the ZnO that was processed in pure nitrogen atmosphere without hydrogen and oxygen, the material has a Zn 2p 3/2 core level binding energy at 1021.3 eV shifted by 0.2 eV with reference to the as-received sample. Its VBM shifts to 2.44 eV from 2.37 eV with the same reference. Such a substantial downwards band bending further supports the notion of accumulation layer formation. Nitrogen is an active acceptor[31] and is therefore unlikely to contribute electrons to the surface if they are successfully doped into the as-prepared material. The downward band bending for this material suggests that under low oxygen vapour pressure, oxygen vacancies may form and act as active donors to contribute electrons near the surface. The electronic transition between the defect state and the downwards band bending region gives rise to the high energy green emission.[32] While the presence of nitrogen creates a low oxygen vapor pressure environment, such that oxygen vacancies are preferably formed, on the other hand, XPS suggested that the nitrogen does not act as a defect level in contributing to the green emission.

It is believed that the donor defects would likely contribute to a downward band bending at the low index surfaces, such as (0001), (000–1), (10–10) as they are thermodynamically stable as compared to other crystal surfaces.[16,25,33] They are also the favorable surfaces of the as-grown crystals. Therefore, a downward surface band bending is mainly contributed to by the donor defects.

Conclusions

In conclusion, we have determined the core level binding energy as well as the VBM of the materials with different specific defects. For the ZnO with Type I defects, both the core level and the valence band shift to higher binding energies, indicating a further downwards band bending due to the formation of an accumulated layer of electrons. The presence of electrons is attributed to the donor concentration and the localized oxygen vacancies near the surface act as Type I defects. The defect state in the downwards bending region is responsible for the observed high energy green emission. On the other hand, the Zn 2p 3/2 core level binding energy for the ZnO with Type II defects shifts to lower binding energy while the VBM shifts to higher binding energy. It shows that the shallower region probed by the Zn 2p 3/2 core level has an increasing concentration of acceptors such as zinc vacancies, which partially compensate to the existing accumulated layers. The formation of higher concentration of oxygen vacancies occurs at a deeper depth ($\sim$81.8 nm) due to the relatively fast cooling rate. These oxygen vacancies are the Type II defects, rendering the low energy green emission. The location of oxygen vacancies as shown in the results determines the characteristic green emissions with different energies, as observed.

Acknowledgements

One of the authors (Y. Y. Tay) would like to thank Singapore Millennium Foundation (SMF) for the scholarship. This research is supported by Australian Research Council Discovery Program No. DP0988687. The authors would like to thank Prof. T. Norby for valuable discussions.

References

1 A. B. Djurišić and Y. H. Leung, *Small*, 2006, **2**, 944.
2 U. Ozgur, Y. I. Alivov, C. Liu, A. Teke, M. A. Reshchikov, S. Dogan, V. Avrutin, S. J. Cho and H. Morkoc, *J. Appl. Phys.*, 2005, **98**, 041301.
3 X. Fang, Y. Bando, U. K. Gautam, T. Zhai, H. Zeng, X. Xu, M. Liao and D. Golberg, *Crit. Rev. Solid State Mat. Sci.*, 2009, **34**, 190–223.
4 A. Tsukazaki, A. Ohtomo, T. Kita, Y. Ohno, H. Ohno and M. Kawasaki, *Science*, 2007, **315**, 1388–1391.
5 T. Dietl, H. Ohno, F. Matsukura, J. Cibert and D. Ferrand, *Science*, 2000, **287**, 1019.
6 X.-S. Fang, C.-H. Ye, L.-D. Zhang, Y. Li and Z.-D. Xiao, *Chem. Lett.*, 2005, **34**, 436.
7 P. Sharma, A. Gupta, K. V. Rao, J. F. Owens, R. Sharma, R. Ahuja, J. M. O. Guillen, B. Johansson and G. A. Gehring, *Nat. Mater.*, 2003, **2**, 673.
8 Y. Yan, S. B. Zhang and S. T. Pantelides, *Phys. Rev. Lett.*, 2001, **86**, 5723.
9 A. B. Djurišić, Y. H. Leung, K. H. Tam, Y. F. Hsu, L. Ding, W. K. Ge, Y. C. Zhong, K. S. Wong, W. K. Chan, H. L. Tam, K. W. Cheah, W. M. Kwok and D. L. Phillips, *Nanotechnology*, 2007, **18**, 095702.
10 K. Vanheusden, C. H. Seager, W. L. Warren, D. R. Tallant and J. A. Voigt, *Appl. Phys. Lett.*, 1996, **68**, 403.

11 A. van Dijken, E. A. Meulenkamp, D. Vanmaekelbergh and A. Meijerink, *J. Lumin.*, 2000, **90**, 123.
12 A. F. Kohan, G. Cedar, D. Morgan and C. G. Van de Walle, *Phys. Rev. B: Condens. Matter Mater. Phys.*, 2000, **61**, 15019.
13 M. Liu, A. H. Kitai and P. Mascher, *J. Lumin.*, 1992, **54**, 35.
14 D. C. Giancoli, *Physics Scientists & Engineers with Modern Physics*, Prentice Hall, New Jersey, 2000.
15 A. Ghosh, N. G. Deshpande, Y. G. Gudage, R. A. Joshi, A. A. Sagade, D. M. Phase and R. Sharma, *J. Alloys Compd.*, 2009, **469**, 56.
16 W. Göpel and U. Lampe, *Phys. Rev. B: Condens. Matter*, 1980, **22**, 6447.
17 Y. Y. Tay, T. T. Tan, F. Boey, M. H. Liang, J. Ye, Y. Zhao, T. Norby and S. Li, *Phys. Chem. Chem. Phys.*, 2010, **12**, 2373.
18 Y. M. Chiang, D. Birnie III and W. David Kingery, *Physical Ceramics: Principles for Ceramic Science and Engineering*, John Wiley & Sons, INC., United States of America, 1997.
19 T. B. Massalski, *Binary Alloy Phase Diagrams*, ASM International, Ohio, 2nd edn, 1992, vol. 3.
20 S. A. Chambers, T. Droubay, T. C. Kaspar and M. Gutowski, *J. Vac. Sci. Technol., B*, 2004, **22**, 2205.
21 V. E. Henrich and P. A. Cox, *The Surface Science of Metal Oxides*, Cambridge University Press, Cambridge, UK, 1994.
22 E. Böhmer, F. Siebke and H. Wagner, *Fresenius J. Anal. Chem.*, 1997, **358**, 210.
23 Y.-J. Lin and C.-L. Tsai, *J. Appl. Phys.*, 2006, **100**, 113721.
24 R. Schlaf, P. G. Schroeder, M. W. Nelson, B. A. Parkinson, P. A. Lee, K. W. Nebesny and N. R. Armstrong, *J. Appl. Phys.*, 1999, **86**, 1499.
25 B. J. Coppa, C. C. Fulton, P. J. Hartlieb, R. F. Davis, B. J. Rodriguez, B. J. Shields and R. J. Nemanich, *J. Appl. Phys.*, 2004, **95**, 5856.
26 S. Tanuma, C. J. Powell and D. R. Penn, *Surf. Interface Anal.*, 1994, **21**, 165.
27 D. Briggs and M. P. Seah, *Practical Surface Analysis by Auger and X-Ray Photoelectron Spectroscopy*, John Wiley & Sons Ltd., Chichester, 1st edn, 1983.
28 G. D. Mahan, *J. Appl. Phys.*, 1983, **54**, 3825.
29 M. V. Ganduglia-Pirovano, M. Scheffler, A. Baraldi, S. Lizzit, G. Comelli, G. Paolucci and R. Rosei, *Phys. Rev. B: Condens. Matter Mater. Phys.*, 2001, **63**, 205415.
30 J. Lahiri, S. Senanayake and M. Batzill, *Phys. Rev. B: Condens. Matter Mater. Phys.*, 2008, **78**, 155414.
31 D. C. Look, G. C. Farlow, P. Reunchan, S. Limpijumnong, S. B. Zhang and K. Nordlund, *Phys. Rev. Lett.*, 2005, **95**, 225502.
32 W. Göpel, *Surf. Sci.*, 1977, **62**, 165.
33 A. Wander, F. Schedin, P. Steadman, A. Norris, R. McGrath, T. S. Turner, G. Thornton and N. M. Harrison, *Phys. Rev. Lett.*, 2001, **86**, 3811.